HHS Public Access

Author manuscript

*Ophthalmic Physiol Opt*. Author manuscript; available in PMC 2019 September 16.

Published in final edited form as:

*Ophthalmic Physiol Opt*. 2018 September ; 38(5): 525–537. doi:10.1111/opo.12581.

# Binocular contrast summation and inhibition depends on spatial frequency, eccentricity and binocular disparity

**Dr. Concetta F Alberti** and **Peter J Bex**

Department of Psychology, Northeastern University, Boston, USA

## Abstract

**Purpose—**When central vision is compromised, visually-guided behaviour becomes dependent on peripheral retina, often at a preferred retinal locus (PRL). Previous studies have examined adaptation to central vision loss with monocular 2D paradigms, whereas in real tasks, patients make binocular eye movements to targets of various sizes and depth in 3D environments.

**Methods—**We therefore examined monocular and binocular contrast sensitivity functions with a 26-AFC (alternate forced choice) band-pass filtered letter identification task at 2° or 6° eccentricity in observers with simulated central vision loss. Binocular stimuli were presented in corresponding or non-corresponding stereoscopic retinal locations. Gaze-contingent scotomas (0.5° radius disks of pink noise) were simulated independently in each eye with a 1000Hz eye tracker and 120Hz dichoptic shutter glasses.

**Results—**Contrast sensitivity was higher for binocular than monocular conditions, but only exceeded probability summation at low-mid spatial frequencies in corresponding retinal locations. At high spatial frequencies or non-corresponding retinal locations, binocular contrast sensitivity showed evidence of interocular suppression.

**Conclusions—**These results suggest that binocular vision deficits may be underestimated by monocular vision tests and identify a method that can be used to select a PRL based on binocular contrast summation.

### Keywords

binocular summation; contrast sensitivity; peripheral vision; binocular inhibition; disparity

## Introduction

People with damaged foveae, as is the case in most patients with late-stage age-related macular degeneration (AMD), must use peripheral retina for viewing, known as the Preferred Retinal Locus (PRL) when a single location is dominant. The function of the PRL in AMD patients has generally been measured monocularly, and in the better eye, with simple tasks such fixation and perimetry dot detection (for review see [1]), or with complex tasks such as reading [2] and face perception.[3] However, both eyes are typically used for

**Corresponding author:** Concetta Alberti, conce.alberti@gmail.com.

Disclosures: The author CFA reports no conflicts of interest and has no proprietary interest in any of the materials mentioned in this article. The author PJB reports: Adaptive Sensory Technology, Personal Financial Interest; Adaptive Sensory Technology, Patent.

everyday activities and require the detection of targets at a range of sizes, contrasts and depths. The use of a PRL has rarely been investigated under these conditions. Where binocular vision has been studied, it has been shown that best monocular vision may underestimate the vision of the weaker eye [4] because the worse eye may be suppressed, [5–8] that stereoacuity is impaired, [8] and that fixation patterns differ from those measured under monocular conditions. [9] These findings severely limit the conclusions that can be drawn from studies of monocular vision.

In normally-sighted observers, binocular vision has been studied extensively at the fovea and it is well-known that binocular visual function depends on a range of stimulus and task factors. [10] The simplest demonstration of binocular function is the comparison of detection thresholds under monocular and binocular viewing conditions. In central vision of healthy eyes, binocular contrast sensitivity is typically greater than the monocular contrast sensitivity of either eye and a stimulus can sometimes be detected binocularly when its contrast is too low to be detected by either of the two eyes independently. This phenomenon is known as binocular contrast summation. [11–33] A binocular contrast summation factor of $\sqrt{2}$ is predicted in single channel systems with either linear summation of correlated signals and independent noise from each eye [12]; or with a squaring non-linearity prior to linear combination. [17] Binocular summation may differ at and above contrast detection threshold [34, 35] and suprathreshold models often involve a summation stage and one or more gain control exponents; these stages can produce summation above $\sqrt{2}$. [36–41] These models are relevant to healthy participants whose monocular foveal contrast sensitivity is similar in each eye. Previous results have demonstrated that binocular contrast summation may be reduced in older subjects [42, 43] or in peripheral visual field.[44]

Furthermore, when interocular contrast sensitivity is dissimilar, for example with cataract, [45] refractive error, [46, 47] amblyopia, [48–50] or age-related macular degeneration, [51] binocular contrast sensitivity may be worse than the best monocular contrast sensitivity of either eye. Within the computational framework described above, a lack of binocular summation can arise from interocular suppression, [52] however these approaches do not account for binocular contrast summation factors that are less than 1, i.e., inhibition.

When central vision is intact, visual targets of interest are imaged at the fovea of both eyes and consequently have zero retinal disparity. Objects at depth planes that differ from that of the foveated target are imaged at non-corresponding retinal locations, either with crossed (positive) or uncrossed (negative) disparity for objects that are closer to or further from the horopter, respectively. Within a volume of space around the horopter known as Panum's Fusional Area, objects with crossed or uncrossed disparity are seen as single, in depth [53] and at full contrast. [39] These observations require phase/disparity-dependent binocular gain control that modulates the apparent phase and contrast of the cyclopean image. [39, 54] In the present manuscript, we extend these findings to examine binocular contrast summation under conditions that are more relevant to people with central vision loss. We examine monocular and binocular contrast sensitivity as a function of spatial frequency, retinal eccentricity and retinal disparity.

## Methods:

### Participants

For 10 participants (age range= 19–35 years, mean = 24.1 years), we recorded the contrast sensitivity functions monocularly and binocularly in corresponding and non-corresponding retinal disparities at 2° eccentricity. One subject was author CA; two subjects were experienced psychophysical observers; and seven subjects were undergraduate students, naive to the purposes of the study, who had no previous experience with psychophysical research and completed the study for course credit. Five Subjects (two experienced and three naive observers who completed the 2° eccentricity experiment) repeated both the binocular and monocular conditions at 6° eccentricity in corresponding and non-corresponding retinal disparities. The same 10 subjects (three experienced and seven naive observers) completed a monocular control experiment. All participants passed binocular fusion Worth 4 dot screening tests (www.bernell.com/category/1064) and had normal range stereovision (Titmus Fly SO-001 StereoTest, www.stereooptical.com/product/fly/), (mean stereoacuity= 67 arcsecs). The study was approved by the Institutional Review Board at Northeastern University and conformed with the Declaration of Helsinki.

### Apparatus:

Stimuli were generated on a PC using MathWorks MATLAB software (www.mathworks.com/matlabcentral/) with functions from the Psychtoolbox (www.psychtoolbox.org) [55, 56] and presented on an Asus VG248QE LCD monitor with screen resolution 1920×1080 pixels at 120Hz and a mean luminance of 240 cd/m$^2$, at 50 cm viewing distance. Shutter glasses (Nvidia GeForce 3D Vision, www.nvidia.com/object/3d-vision-main.html) were used to control stereoscopic stimulus presentation at 60 Hz per eye. The monitor was gamma-corrected to obtain linear output across RGB values and a bit-stealing algorithm [57] was used to obtain 9.6 bits luminance resolution. Subpixel resolution via the graphics card provided a spatial positioning accuracy of .004 pixel, corresponding to a stereo display resolution of 0.2 arcsec.

A gaze-contingent scotoma was simulated [58] independently for each eye by positioning a circular Gaussian ($\sigma$=0.5°) windowed patch of 100% contrast pink noise at the point of gaze of each eye on the computer display. The location of each eye was recorded with an EyeLink II eyetracker (www.sr-research.com/products/eyelink-ii) at 500Hz per eye.

### Stimuli:

Contrast sensitivity was measured using a modified quickCSF algorithm [59] that controlled the spatial frequency and contrast of 26 band-pass filtered Sloan font letters. We elected to use the full alphabet instead of a subset of letters because reducing the guessing rate greatly improves the efficiency of testing, [60] this avoids forcing the subject to repeat a response when a target that is not in the subset is reported, and because identification differences are not avoided with subsets [61–63] (see Hamm *et al.* [64] for recent review). The quickCSF algorithm exploits the known 2D shape of the CSF, which conforms to an asymmetric log-parabola with four parameters [65]: peak gain, peak spatial frequency, low spatial frequency bandwidth and high spatial frequency bandwidth, and assumes the logarithm of the slope of

the underlying psychometric function is constant across spatial frequencies.[66, 67] Each trial, a one-step ahead search for all combinations of spatial frequency and contrast, then elects the stimulus that maximises the expected information gain. [68, 69] The quickCSF algorithm effectively simulates the next trial and evaluates responses to possible stimuli for their expected effects on the posterior. With this method regions of the stimulus space that are not likely to be useful to build the 2D contrast sensitivity function are avoided and trials at all spatial frequencies and contrasts contribute to the estimate of the underlying psychometric function at any spatial frequency. The quickCSF specifies the spatial frequency and contrast of the letter on each trial, each letter is digitally band-pass filtered with a raised cosine log filter with a peak spatial frequency of five cycles per letter [70] and one octave bandwidth. The letters were scaled in size to produce the required spatial frequency on screen.

The binocular locations of the letters were either in corresponding (0° disparity), or non-corresponding retinal locations via crossed and uncrossed disparities. The horizontal disparity was scaled with stimulus size to maintain a ¼ cycle (90° phase) shift of the peak spatial frequency. This constant quadrature phase shift ensured constant depth sensitivity, [71] contrast summation [72] and perceived contrast [39] across spatial frequencies. Corresponding and non-corresponding (crossed or uncrossed) conditions were randomly interleaved within a run.

### Procedure:

Observers were instructed to align the simulated scotoma between two vertically aligned dots on the screen and then to click a mouse button to initiate a trial. Each trial began with a Nonius square presented 2° (Experiment 1) or 6° (Experiment 2) below fixation on separate runs. The lower visual field was chosen for PRL location as it is often selected as a PRL training location in low vision rehabilitation, primarily because it may prevent upcoming text from falling into the scotoma during reading. [73–76]

The Nonius square was twice the size of the unfiltered target letter to provide an indication of the size / spatial frequency of the upcoming target. Participants were required to fuse the Nonius squares presented within the Panum's fusional areas and, once fusion was achieved, click a mouse button to trigger the presentation of the target letter. The target letter was randomly selected from the 26 letters of the alphabet and was presented in the centre of the Nonius square at a spatial frequency and contrast determined by the quickCSF algorithm described in the Stimuli section. The letter was presented within a Gaussian temporal envelope with standard deviation of 250 ms. This was followed by the response screen that contained all 26 letters of the alphabet arranged along the top of the screen. The observer's task was to report the identity of the target by clicking on the corresponding letter in the response screen.

On monocular trials, the non-tested eye was occluded with an eye patch. On binocular trials, the target letter was the same identity, spatial frequency and contrast in both eyes. On corresponding trials, the letters were presented in the same position in the left eye and right eye. On non-corresponding trials, the letters were presented at a disparity corresponding to ¼ cycle (90° phase shift) of the peak spatial frequency of the letter target. The sign of the disparity was randomised across trials.

Eight CSFs were estimated within one session in a randomised order (four monocular CSFs and four binocular CSFs, two for stimuli in corresponding positions and two for stimuli in non-corresponding positions). Each CSF was measured with 50 trials. We derived monocular thresholds for each eye and binocular thresholds at each spatial frequency as well as two summary statistics from the CSF: (i) area under log CSF (AULCSF) which represents the overall contrast sensitivity of the patient, [77] and (ii) CSF Acuity, the high spatial-frequency cutoff corresponding to the highest spatial frequency target than can be identified at full contrast.

## Data Analysis

In order to quantify binocular summation, standard practice is to report the ratio of binocular and monocular detection thresholds[11–19, 26, 28] under the assumption that the two eyes have the same detection threshold. However, when contrast sensitivity differs between the two eyes, as is the case for most clinical populations [45–51], the two eyes have different detection thresholds. We therefore computed predicted binocular target detection probability based on the underlying observed monocular target detection probabilities. We then compared the predicted binocular target detection probability with the observed binocular target detection probability at each spatial frequency. From each monocular and binocular quickCSF, we extracted contrast sensitivity at 16 spatial frequencies, at evenly spaced log steps between 0.5 and 16 c/deg. This range was selected because of the physical constraints of the apparatus at the 50cm viewing distance and because of the low sensitivity to spatial frequencies above 16 c/deg in peripheral visual field. To examine binocular summation, we first calculated the contrast detection threshold for the binocular CSF as the reciprocal of contrast sensitivity at each spatial frequency. The quickCSF assumes a Weibull psychometric function:

$$P = 1 - (1 - \gamma) * e^{-(C/\alpha)^{\beta}} \quad \text{[Equation 1]}$$

where $C$ is stimulus contrast, $\alpha$ is threshold contrast, $\gamma$ is guessing rate ($\gamma$ =0.03 for our 26-AFC task) and $\beta$ is the slope ($\beta$= 2;[66]). For our 26AFC task, the binocular contrast detection threshold corresponds to the signal contrast at which the probability of detection ($P_{Observed\ Binocular}$) is 0.643. For each binocular contrast threshold, we calculated the probability of target detection by the left eye and by the right eye based on their monocular contrast sensitivity at the same spatial frequency. For each spatial frequency, the probability of monocular target detection (P) can be directly estimated at the binocular contrast threshold (C) given the monocular threshold ($\alpha$), where $\gamma$ and $\beta$ are fixed. [78, 79]

The expected probability of binocular detection ($P_{Expected\ Binocular}$) based on the probabilistic summation of independent monocular signals is given by:

$$P_{\text{Expected Binocular}} = P_{\text{Left eye}} + P_{\text{Right eye}} - \left(P_{\text{Left eye}} * P_{\text{Right eye}}\right) \quad \text{[Equation 2]}$$

where $P_{\text{Left eye}}$ and $P_{\text{Right eye}}$ are the detection probabilities for the left and right eye. The ratio of $P_{Observed\ \text{Binocular}} / P_{\text{Expected binocular}}$ provides an estimate of the binocular summation factor for each spatial frequency. A ratio of 1 indicates simple probability summation – i.e. the observed binocular detection threshold is equal to the threshold predicted by independent detection by the left eye and right eye. A ratio greater than 1 provides evidence for binocular contrast summation, and a value lower than 1 shows evidence of binocular inhibition.

Parametric analyses were used throughout the paper; analyses were run using lme package in R.2.5 (www.rdocumentation.org/packages/nlme/versions/3.1-137/topics/lme). Statistical comparisons were Bonferroni corrected for multiple comparisons.

## Results

### Contrast Sensitivity

Figure 1 shows monocular (light grey) and binocular (dark grey) contrast sensitivity functions for corresponding (left column) and non-corresponding (right column) stimuli at 2° (top row) and 6° (bottom row) eccentricity. Contrast sensitivity was higher at 2° than 6° eccentricity in both corresponding ($F_{(1, 124)}$= 507, p<0.001) and non-corresponding ($F_{(1, 124)}$= 506, p<0.001) conditions, in good agreement with many previous studies. [80] At both 2° and 6° eccentricities, binocular contrast sensitivity exceeded monocular contrast sensitivity for both corresponding (2° $F_{(1,279)}$= 573, p<0.001; 6° $F_{(1,124)}$= 410, p<0.001) and non-corresponding (2° $F_{(1,279)}$= 182, p<0.001; 6° $F_{(1,124)}$= 78, p<0.001) conditions. These findings confirm previous studies [16, 17] and extend them to a full spatial frequency range, to para-central visual field and to stimuli in depth.

Figure 2 shows monocular (light grey) and binocular (dark grey) acuity for corresponding (left column) and non-corresponding (right column) stimuli at 2° (top row) and 6° (bottom row) eccentricity. Monocular acuities are replotted for comparison in both columns. Acuity was higher at 2° than 6° eccentricity in both corresponding ($F_{(1,13)}$=22, p<0.001), non-corresponding ($F_{(1,13)}$=43, p<0.001) and monocular conditions ($F_{(1,13)}$=28, p<0.001), in good agreement with previous studies. [80] At both 2° and 6° eccentricities, binocular and monocular acuity did not significantly differ for either corresponding (2° $F_{(1,9)}$=3.82, p=0.08; 6° $F_{(1,4)}$=5.17, p=0.08) or non-corresponding (2° $F_{(1,9)}$=3.74, p=0.08; 6° $F_{(1,4)}$=0.02, p=0.88) conditions.

Figure 3 shows monocular (light grey) and binocular (dark grey) AULCSF for corresponding (left column) and non-corresponding (right column) stimuli at 2° (top row) and 6° (bottom row) eccentricity. Monocular AULCSF is replotted for comparison in both columns. AULCSF was higher at 2° than 6° eccentricity in both corresponding ($F_{(1,4)}$=25, p=0.007), non-corresponding ($F_{(1,4)}$=39, p=0.003) and monocular conditions ($F_{(1,4)}$=47, p=0.002), in good agreement with previous studies. [80] At both 2° and 6° eccentricities, binocular contrast sensitivity exceeded monocular contrast sensitivity for both corresponding (2° $F_{(1,9)}$=77, p<0.001; 6° $F_{(1,4)}$=74, p<0.001) and non-corresponding (2° $F_{(1,9)}$=21, p=0.0012; 6° $F_{(1,4)}$=10, p=0.03) conditions.

## Binocular Summation

Figure 4 shows binocular summation ratios ($P_{Observed\ \mathrm{Binocular}} / P_{\mathrm{Expected\ binocular}}$) for corresponding (left column) and non-corresponding (right column) binocular stimuli at 2° (top row) and 6° (bottom row) eccentricity.

In the corresponding conditions, binocular contrast summation exceed probability summation at both 2° eccentricity ($F_{(1, 279)}$= 75, p<0.001) and at 6° eccentricity ($F_{(1, 124)}$= 23, p<0.001). There was a significant interaction of spatial frequency and the type of ratio (observed versus predicted) at both 2° ($F_{(15, 279)}$= 2.06, p=0.01) and 6° ($F_{(15,124)}$= 2.67, p=0.0015) eccentricities, indicating that binocular summation is highly dependent on spatial frequency. Asterisks show the significance of pairwise t-tests and indicate which spatial frequencies showed, after correction for multiple comparisons, significant evidence of binocular summation (summation factor >1) or interocular inhibition (summation factor <1).

In the non-corresponding condition, binocular contrast thresholds were significantly below probability summation at both 2° eccentricity ($F_{(1,279)}$= 16, p<0.001) and at 6° eccentricity ($F_{(1,124)}$= 42, p<0.001). There was no significant interaction at 2° eccentricity ($F_{(15,279)}$= 1.42, p=0.13) but the interaction was significant at 6° eccentricity ($F_{(15,124)}$= 2.07, p=0.015) suggesting that at some spatial frequencies, contrast detection thresholds are consistent with binocular contrast inhibition. Asterisks show the significance of pairwise t-tests and indicate spatial frequencies that showed significant evidence of interocular inhibition (summation factor <1).

These results confirm and extend previous studies and provide evidence for binocular contrast summation. [36–38] However, the present results demonstrate that such contrast summation is present only at low and intermediate spatial frequencies and only for stimuli in corresponding retinal locations.

## Crosstalk control

When using liquid crystal shutter glasses to separate stereo half-images, interocular “cross-talk” can occur. It is therefore possible that the binocular contrast summation we observe for corresponding but not non-corresponding stimuli could arise from additive cross talk in successive displays. Simmons and Kingdom [81] report that at low stimulus contrasts (i.e., close to detection threshold, as in the present study) this cross-talk was undetectable. [19, 81] Furthermore, Figure 1 and Figure 4 show a strong spatial frequency dependence of correspondence, suggesting that the effect is not fully attributable to display cross-talk. Nevertheless, since TFT and LCD displays show non-linearities, [82, 83] to test if cross-talk contributed to our results, we compared the corresponding versus non-corresponding conditions at 2° eccentricity when the stimulus was viewed only monocularly, with the non-tested eye covered by an eye patch. In the corresponding condition, alternate fames (not presented to the test eye), contained an identical stimulus. In the non-corresponding conditions, alternate frames (not presented to the test eye), contained a ¼ cycle (90°) phase shifted stimulus. If crosstalk mediated our results, contrast sensitivity should be higher in the corresponding condition. Figure 5 shows monocular CSFs for 10 observers for corresponding and non-corresponding conditions. Contrast sensitivity was not significantly

different between corresponding and non-corresponding conditions at any spatial frequency. We therefore conclude that cross-talk does not account for the differences in binocular and monocular contrast sensitivity in our main experiments.

## Discussion

We measured monocular and binocular contrast sensitivity functions at 2° and 6° eccentricity, with band-pass spatial frequency filtered letter stimuli that were presented in either corresponding or non-corresponding stereoscopic disparities. Consistent with many previous studies, under some conditions, binocular contrast sensitivity exceeded monocular contrast sensitivity by a factor that exceeded probability summation, and therefore provides evidence for binocular visual summation. Extending previous studies, we find that such super-probability summation occurs only at low spatial frequencies, low eccentricities and for corresponding retinal disparities. For non-corresponding stimuli, binocular contrast sensitivity does not exceed probability summation, and at high spatial frequencies there is evidence of interocular inhibition.

We found contrast summation in the central and para-central region only in the 0-disparity (corresponding) condition and at the lowest spatial frequencies, while contrast inhibition was found at high spatial for the non-corresponding condition. We found an average 1.4-fold increase in contrast sensitivity in a 26-AFC discrimination task in the corresponding condition with respect to the increase expected from simple probability summation alone. For low-intermediate spatial frequencies, contrast summation is slightly less at 6° than at 2° eccentricity. These results are in good agreement with earlier studies on binocular summation, where a 1.4 factor increase was observed in monocular detection contrast thresholds for sine-wave gratings compared to binocular contrast thresholds [12, 16]. Under standard explanations of these data, each monocular channel contains internal noise which determines signal detection threshold. However, since the standard error of n measurements of noisy processes will decrease in proportion to sqrt(n), with two channels an increase in sensitivity of $\sqrt{2}$=1.41 is expected. [11, 84]

In situations of non-zero-disparity (with or without diplopia), previous studies of foveal vision have reported that binocular summation fails. [18, 72, 85] Accordingly to Rose *et al.*, [72] there is a range up to 3–4 degrees disparity for binocular summation to occur. As disparity increases, binocular summation decreases, such that at large disparities contrast summation was near 1.2, close to the value expected from probability summation alone. They also reported that disparity range limit was scaled with stimulus size to support binocular summation. In our experiment disparity was scaled, with stimulus size and spatial frequency in the range of 0.5° at 0.5 c/deg to 0.0625° at 16 c/deg; these values should be within the range suggested by Rose *et al.* [72]

Our results show that binocular visual acuity was higher than monocular visual acuity, however the effect was not significant. These results are consistent with previous studies of visual acuity which have reported relatively small (c. 10%) increases in binocular acuity [86–88] and a lack of any benefit in visual acuity at the location of a PRL in AMD patients. [35] In comparison, the AULCSF, an overall estimate of contrast sensitivity, was significantly higher under binocular viewing conditions, again consistent with previous studies. [89] This

result suggests that while acuity may not be improved at a binocular PRL [35], contrast sensitivity may demonstrate a benefit from PRL training.

In most cases of pathological central vision loss, the scotoma size and location is asymmetrical. This complicates the selection of a PRL for best binocular function. Since contrast sensitivity decreases approximately linearly along each meridian with increases in eccentricity, [20–33] a PRL closest to the fovea should support best visual function. Baldwin *et al.* [89] proposed a witch's hat model to describe this function:

$$S = log_{10}\left(\frac{10^{-m_1 E}}{10^{(m_1 - m_2)v} + 10^{(m_1 - m_2)E}}\right) + K \quad \text{[Equation 3]}$$

Where $S$ is contrast sensitivity in dB, $E$ is eccentricity in degrees, $m_1$ and $m_2$ control the slope of the first and second limbs of the function (with the constraint that $m_1 \leq m_2$), $v$ determines the location of the knee point and $K$ controls the vertical position of the function. Baldwin *et al.* [89] provide estimates of $m_1$, $m_2$, $v$ and $K$ for normally-sighted observers.

However, since such summation can provide a contrast sensitivity benefit of at least a factor of 1.4, depending on spatial frequency and disparity, best overall visual function may depend on the relative sizes of the scotomas in each eye rather than on best visual acuity (Bernard and Chung, 2018). Our results suggest that Equation 3 can be used to estimate the highest monocular contrast sensitivity in each eye, based on the size of the scotoma in that eye. In order to select the best overall function, it is relatively straightforward to compare *monocular* sensitivity at the lower eccentricity of the better eye with *binocular* sensitivity at the greater eccentricity of the worse eye. If sensitivity in the eye with the smaller scotoma exceeds sensitivity of the eye with the larger scotoma by more than a factor of 1.4, then this monocular location should be selected. Otherwise the more eccentric binocular location should be selected.

## Limitations

In addition to reporting the ratios of acuity and AULCSF to estimate binocular summation, we implemented a simple, classic model of probability summation that is based on high threshold theory for detection of signal in independent channels. While this approach is limited for supra-threshold binocular vision [90], its assumptions are reasonable at contrast detection threshold. [91] We also assumed that the underlying psychometric function was a Weibull function with a fixed slope. [66, 67] The slope parameter affects the predicted monocular detection probability, and we do not have sufficient data to constrain the slope at all spatial frequencies in the present study. However, predicted binocular summation at each spatial frequency was close to the values obtained for summation of the AULCSF. In more contemporary models of binocular function, summation is linear and determined by early non-linearities, while noise is late and additive. We therefore implemented the model proposed by [39, 40] and the results, shown in the Appendix, are in good agreement with the results reported with classic methods.

The present experiments were conducted in young healthy observers and we simulated central vision loss with a gaze-contingent scotoma. In instances of pathological central vision loss, there is evidence of longitudinal plasticity, reorganisation and attentional changes that might influence sensitivity and binocular summation. [92] Furthermore, the magnitude of binocular summation decreases with age.[44] Additionally, as we tested only in the inferior visual field, which is frequently the target for PRL training, it is possible that binocular summation may vary with visual field location. We also used an eye patch to occlude the untested eye, as is common practice, for monocular threshold measurement. However, given that binocular summation is affected by mean luminance [84], different results may be obtained with a mean luminance target in the untested eye. Before our findings can be generalised to low vision rehabilitation for AMD patients, therefore, further testing involving visually impaired populations is necessary to support conclusions about binocular summation and best eccentric binocular location.

## Acknowledgements:

This work was supported by the National Institutes of Health (NIH grant HHS/1K99EY026130).

## Appendix

For comparison with alternative models of binocular contrast summation we calculated the Summation Ratio (SR) using Meese and Summer's (2009) method:

$$SR = 20\log_{10}\left(\text{threshold}_{\text{monocular}}/\text{threshold}_{\text{binocular}}\right)$$

Figure A1 expresses the summation ratio in decibels (dB). Since a larger ratio corresponds to a larger summation level, Figure A1 confirms the trend observed using the Binocular Summation Factor in Figure 4.

## References

1. Crossland MD, Jackson M & Seiple WH. Microperimetry: A review of fundus related perimetry. Optom Reports 2012;2:11–15.
2. Nilsson UL, Frennesson C & Nilsson SE. Location and stability of a newly established eccentric retinal locus suitable for reading, achieved through training of patients with a dense central scotoma. Optom Vis Sci 1998;75:873–878. [PubMed: 9875992]
3. Seiple W, Rosen RB & Garcia PM. Abnormal fixation in individuals with age-related macular degeneration when viewing an image of a face. Optom Vis Sci 2013;90:45–56. [PubMed: 23238260]
4. Podbielski DW, Reyes SV & Markowitz SN. The worse eye is not as bad as it seems to be in amd cases. Can J Ophthalmol 2013;48:381–385. [PubMed: 24093184]
5. Quillen DA. Effect of unilateral exudative age-related macular degeneration on binocular visual function. Arch Ophthalmol 2001;119:1725–1726. [PubMed: 11709032]
6. Tarita-Nistor L, Gonzalez EG, Markowitz SN & Steinbach MJ. Binocular interactions in patients with age-related macular degeneration: Acuity summation and rivalry. Vision Res 2006;46:2487–2498. [PubMed: 16545856]
7. Faubert J & Overbury O. Binocular vision in older people with adventitious visual impairment: Sometimes one eye is better than two. J Am Geriatr Soc 2015;48:375–380.

8. Cao KY & Markowitz SN. Residual stereopsis in age-related macular degeneration patients and its impact on vision-related abilities: A pilot study. J Optom 2014;7:100–105. [PubMed: 24766867]
9. Kabanarou SA, Crossland MD, Bellmann C, Rees A, Culham LE & Rubin GS. Gaze changes with binocular versus monocular viewing in age-related macular degeneration. Ophthalmology 2006;113:2251–2258. [PubMed: 16996593]
10. Blake R & Wilson H. Binocular vision. Vision Res 2011;51:754–770. [PubMed: 20951722]
11. Pirenne MH. Binocular and uniocular thresholds of vision. Nature 1943;152:698–699.
12. Campbell FW & Green DG. Monocular versus binocular visual acuity. Nature 1965;208:191–192. [PubMed: 5884255]
13. Blake R & Fox R. The psychophysical inquiry into binocular summation. Percept Psychophys 1973;14:161–185.
14. Thorn F & Boynton RM. Human binocular summation at absolute threshold. Vision Res 1974;14:445–458. [PubMed: 4422216]
15. Blake R, Sloane M & Fox R. Further developments in binocular summation. Percept Psychophys 1981;30:266–276. [PubMed: 7322802]
16. Legge GE. Binocular contrast summation--i. Detection and discrimination. Vision Res 1984;24:373–383. [PubMed: 6740958]
17. Legge GE. Binocular contrast summation--ii. Quadratic summation. Vision Res 1984;24:385–394. [PubMed: 6740959]
18. Rose D Monocular versus binocular contrast thresholds for movement and pattern. Perception 1978;7:195–200. [PubMed: 652478]
19. Simmons DR & Kingdom FAA. On the binocular summation of chromatic contrast. Vision Res 1998;38:1063–1071. [PubMed: 9666966]
20. Poppel E & Harvey LO, Jr., Light-difference threshold and subjective brightness in the periphery of the visual field. Psychol Forsch 1973;36:145–161. [PubMed: 4770517]
21. Hilz R & Cavonius CR. Functional organization of the peripheral retina: Sensitivity to periodic stimuli. Vision Res 1974;14:1333–1337. [PubMed: 4446364]
22. Koenderink JJ, Bouman MA, Bueno de Mesquita AE & Slappendel S. Perimetry of contrast detection thresholds of moving spatial sine wave patterns. Iii. The target extent as a sensitivity controlling parameter. J Opt Soc Am 1978;68:854–860. [PubMed: 702224]
23. Rovamo J, Virsu V & Nasanen R. Cortical magnification factor predicts the photopic contrast sensitivity of peripheral vision. Nature 1978;271:54–56. [PubMed: 625324]
24. Rovamo J & Virsu V. An estimation and application of the human cortical magnification factor. Exp Brain Res 1979;37:495–510. [PubMed: 520439]
25. Rijsdijk JP, Kroon JN & van der Wildt GJ. Contrast sensitivity as a function of position on the retina. Vision Res 1980;20:235–241. [PubMed: 7385597]
26. Robson JG & Graham N. Probability summation and regional variation in contrast sensitivity across the visual field. Vision Res 1981;21:409–418. [PubMed: 7269319]
27. Wright MJ & Johnston A. Spatiotemporal contrast sensitivity and visual field locus. Vision Res 1983;23:983–989. [PubMed: 6649443]
28. Kelly DH. Retinal inhomogeneity. Ii. Spatial summation. J Opt Soc Am A 1984;1:114–119. [PubMed: 6699747]
29. Johnston A Spatial scaling of central and peripheral contrast-sensitivity functions. J Opt Soc Am A 1987;4:1583–1593. [PubMed: 3625340]
30. Hess RF, Pointer JS & Watt RJ. How are spatial filters used in fovea and parafovea? J Opt Soc Am A 1989;6:329–339. [PubMed: 2926530]
31. Rovamo J, Franssila R & Näsänen R. Contrast sensitivity as a function of spatial frequency, viewing distance and eccentricity with and without spatial noise. Vision Res 1992;32:631–637. [PubMed: 1413547]
32. Foley J, Varadharajan S, Koh CC & Farias M. Detection of gabor patterns of different sizes, shapes, phases and eccentricities. Vision Res 2007;47:85–107. [PubMed: 17078992]
33. Hess RF, Baker DH, May KA & Wang J. On the decline of 1st and 2nd order sensitivity with eccentricity. J Vis 2008;8:1–12.

34. Pardhan S Binocular recognition summation in the peripheral visual field: Contrast and orientation dependence. Vision Res 2003;43:1251–1257.
35. Bernard JB & Chung STL. Visual acuity is not the best at the preferred retinal locus in people with macular disease. Optom Vis Sci 2018 6 6 95(9):829–836. doi: 10.1097/OPX.0000000000001229. [PubMed: 29877902]
36. Ding J & Sperling G. A gain-control theory of binocular combination. Proc Natl Acad Sci U S A 2006;103:1141–1146. [PubMed: 16410354]
37. Meese TS, Georgeson M & Baker DH. Binocular contrast vision at and above threshold. J Vis 2006;6:1224–1243. [PubMed: 17209731]
38. Baker DH & Meese TS. Binocular contrast interactions: Dichoptic masking is not a single process. Vision Res 2007;47:3096–3107. [PubMed: 17904610]
39. Baker DH, Wallis SA, Georgeson MA & Meese TS. Nonlinearities in the binocular combination of luminance and contrast. Vision Res 2012;56:1–9. [PubMed: 22289645]
40. Meese TS & Summers RJ. Neuronal convergence in early contrast vision: Binocular summation is followed by response nonlinearity and area summation. J Vis 2009;9:1–16.
41. Cohn TE & Lasley DJ. Binocular vision: Two possible central interactions between signals from two eyes. Science 1976;192:561–563. [PubMed: 1257791]
42. Schneck ME, Haegerstöm-Portnoy G, Lott LA & Brabyn JA. Monocular vs. Binocular measurement of spatial vision in elders. Optom Vis Sci 2010;87:526–531. [PubMed: 20526225]
43. Pardhan S A comparison of binocular summation in the peripheral visual field in young and older patients. Curr Eye Res 1997;16:252–255. [PubMed: 9088742]
44. Pardhan S & Whitaker A. Binocular summation to gratings in the peripheral field in older subjects is spatial frequency dependent. Curr Eye Res 2003;26:297–302. [PubMed: 12854058]
45. Pardhan S & Gilchrist J. The importance of measuring binocular contrast sensitivity in unilateral cataract. Eye 1991;5:31. [PubMed: 2060667]
46. Pardhan S & Gilchrist J. The effect of monocular defocus on binocular contrast sensitivity. Ophthalmic Physiol Opt 1990;10:33–36. [PubMed: 2330211]
47. Jiménez JR, Ponce A& Anera RG. Induced aniseikonia diminishes binocular contrast sensitivity and binocular summation. Optom Vis Sci 2004;81:559–562. [PubMed: 15252357]
48. Pardhan S & Gilchrist J. Binocular contrast summation and inhibition in amblyopia. the influence of the interocular difference on binocular contrast sensitivity. Doc Ophthalmol 1992;82:239–248. [PubMed: 1303860]
49. Dorr M Binocular summation and suppression of contrast sensitivity in strabismus, fusion and amblyopia. Submitted to *JAMA Ophthalmol*.
50. Pardhan S & Whitaker A. Binocular summation in the fovea and peripheral field of anisometropic amblyopes. Curr Eye Res 2000;20:35–44. [PubMed: 10611713]
51. Valberg A & Fosse P. Binocular contrast inhibition in subjects with age-related macular degeneration. J Opt Soc Am A 2002;19:223–228.
52. Baker DH, Meese TS & Georgeson MA. Binocular interaction: Contrast matching and contrast discrimination are predicted by the same model. Spat Vis 2007;20:397–413. [PubMed: 17716525]
53. Richards W Spatial remapping in the primate visual system. Kybernetic 1968;4:146–156.
54. Ding J, Klein SA & Levi DM. Binocular combination of phase and contrast explained by a gain-control and gain-enhancement model. J Vis 2013;13:13.
55. Brainard DH. The psychophysics toolbox. Spat Vis 1997;10:443–446. [PubMed: 9176954]
56. Pelli DG. The videotoolbox software for visual psychophysics: Transforming numbers into movies. Spat Vis 1997;10:437–442. [PubMed: 9176953]
57. Tyler CW. Colour bit-stealing to enahnce the luminance resolution of digital displays on a single pixel basis. Spat Vis 1997;10:369–377. [PubMed: 9176946]
58. Alberti CF & Bex PJ. Compensatory strategies for independent binocular scotomas in simulated cfl. ARVO Abstract: Invest Ophthalmol Vis Sci; 2015 56(7): 2904–2904.
59. Lesmes LA, Lu ZL, Baek J & Albright TD. Bayesian adaptive estimation of the contrast sensitivity function: The quick csf method. J Vis 2010;10:17 11–21.

60. Hou F, Lesmes L, Bex P, Dorr M & Lu ZL. Using 10AFC to further improve the efficiency of the quick CSF method. J Vis 2015;15:1–18.
61. Alexander KR, Xie W & Derlacki DJ. Visual acuity and contrast sensitivity for individual sloan letters. Vision Res 1997;37:813–819. [PubMed: 9156226]
62. Bennett AG. Ophthalmic test types. A review of previous work and discussions on some controversial questions. Br J Physiol Optic 1965;22:238–271.
63. Ferris FL, III, Freidlin V, Kassoff A, Green SB & Milton RC. Relative letter and position difficulty on visual acuity charts from the early treatment diabetic retinopathy study. Am J Ophthalmol 1993;116:735–740. [PubMed: 8250077]
64. Hamm LM, Yeoman JP, Anstice N & Dakin SC. The Auckland optotypes: An open-access pictogram set for measuring recognition acuity. J Vis 2018;18:13.
65. Watson AB & Ahumada AJ, Jr., A standard model for foveal detection of spatial contrast. J Vis 2005;5:717–740. [PubMed: 16356081]
66. Watson AB & Pelli DG. Quest: A bayesian adaptive psychometric method. Percept Psychophys 1983;33:113–120. [PubMed: 6844102]
67. Lesmes LA, Lu Z-L, Baek J, Tran N, Dosher BA & Albright TD. Developing bayesian adaptive methods for estimating sensitivity thresholds (d′) in yes-no and forced-choice tasks. Front Psychol 2015;6:1070. [PubMed: 26300798]
68. Kujala JV & Lukka TJ. Bayesian adaptive estimation: The next dimension. J Math Psychol 2006;50:369–389.
69. Lesmes LA, Jeon S-T, Lu Z-L & Dosher BA. Bayesian adaptive estimation of threshold versus contrast external noise functions: The quick tvc method. Vision Res 2006;46:3160–3176. [PubMed: 16782167]
70. Solomon JA & Pelli DG. The visual filter mediating letter identification. Nature 1994;369:395–397. [PubMed: 8196766]
71. Schor CM & Wood I. Disparity range for local stereopsis as a function of luminance spatial frequency. Vision Res 1983;23:1649–1654. [PubMed: 6666067]
72. Rose D, Blake R & Halpern DL. Disparity range for binocular summation. Invest Ophthalmol Vis Sci 1988;29:283–290. [PubMed: 3338886]
73. Fletcher DC & Schuchard RA. Preferred retinal loci relationship to macular scotomas in a low-vision population. Ophthalmology 1997;104:632–638. [PubMed: 9111255]
74. Fletcher DC, Schuchard RA & Watson G. Relative locations of macular scotomas near the prl: Effect on low vision reading. J Rehabil Res Dev 1999;36:356–364. [PubMed: 10678458]
75. Guez JE, Le Gargasson JF, Rigaudiere F & O'Regan JK. Is there a systematic location for the pesudo-fovea in patients with central scotoma. Vision Res 1993;33:1271–1279. [PubMed: 8333174]
76. Barraza-Bernal MJ, Ivanov IV, Nill S, Rifai K, Trauzettel-Klosinski S & Wahl S. Can positions in the visual field with high attentional capabilities be good candidates for a new preferred retinal locus? Vision Res 2017;140:1–12. [PubMed: 28778600]
77. Applegate RA, Howland HC, Sharp RP, Cottingham AJ & Yee RW. Corneal aberrations and visual performance after radial keratotomy. J Refract Surg 1998;14:397–407. [PubMed: 9699163]
78. Dubois M, Poeppel D & Pelli DG. Seeing and hearing a word: Combining eye and ear is more efficient than combining the parts of a word. PLoS One 2013;8:e64803. [PubMed: 23734220]
79. Pelli DG. Research note on the relation between summation and facilitation. Vision Res 1987;27:119–123. [PubMed: 3617542]
80. Strasburger H, Rentschler I & Juttner M. Peripheral vision and pattern recognition: A review. J Vis 2011;11:13.
81. Simmons DR & Kingdom FA. Contrast thresholds for stereoscopic depth identification with isoluminant and isochromatic stimuli. Vision Res 1994;34:2971–2982. [PubMed: 7975331]
82. Elze T & Tanner TG. Liquid crystal display response time estimation for medical applications. Med Phys 2009;36:4984–4990. [PubMed: 19994507]
83. Elze T & Tanner TG. Temporal properties of liquid crystal displays: Implications for vision science experiments. PLoS One 2012;7.

84. Gilchrist J & Pardhan S. Binocular contrast detection with unequal monocular illuminance. Ophthalmic Physiol Opt 1987;7:373–377. [PubMed: 3454912]
85. Long GM. The dichoptic viewing paradigm: Do the eyes have it? Psychol Bull 1979;36:391–403.
86. Horowitz MW. An analysis of the superiority of binocular over monocular visual acuity. J Exp Psychol 1949;39:581–596. [PubMed: 15391102]
87. Home R Binocular summation: A study of contrast sensitivity, visual acuity and recognition. Vision Res 1978;18:579–585. [PubMed: 664341]
88. Heravian JS, Jenkins TC & Douthwaite WA. Binocular summation in visually evoked responses and visual acuity. Ophthalmic Physiol Opt 1990;10:257–261. [PubMed: 2216474]
89. Baldwin AS, Meese TS & Baker DH. The attenuation surface for contrast sensitivity has the form of a witch's hat within the central visual field. J Vis 2012;12.
90. Tyler CW & Chen C. Signal detection theory in the 2afc paradigm: Attention, channel uncertainty and probability summation. Vision Res 2000;40:3121–3144. [PubMed: 10996616]
91. Laming D Probability summation—a critique. J Opt Soc Am A 2013;30 300–315.
92. Jones BW, Marc RE & Pfeiffer RL. Retinal degeneration, remodeling and plasticity In: Kolb H F E, Nelson R, editors (ed), Webvision: The organization of the retina and visual system [internet]. Salt Lake City (UT): University of Utah Health Sciences Center; 1995-; 2016.

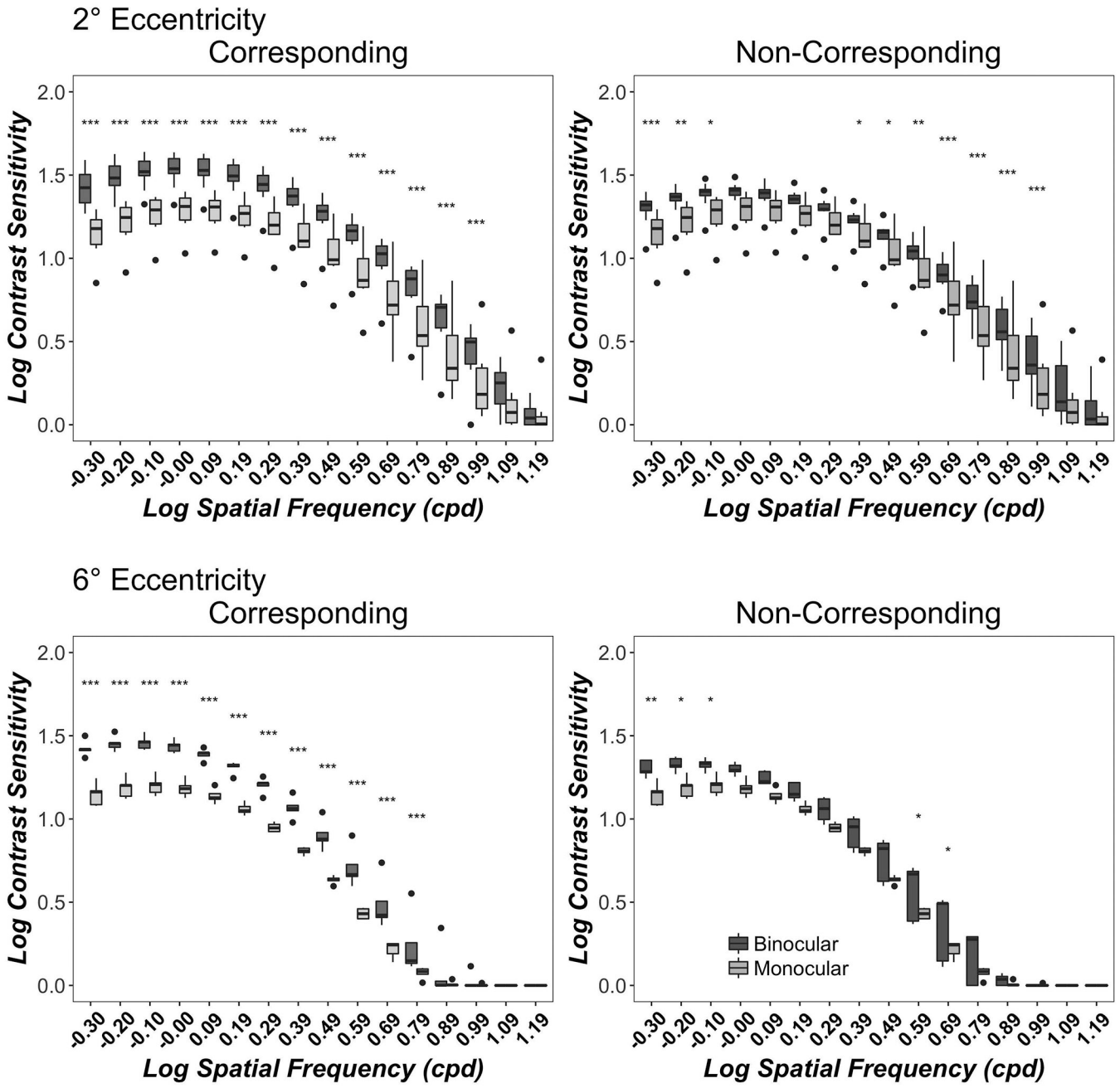


**Figure 1.**

Monocular and Binocular Contrast Sensitivity Functions. Data show contrast sensitivity from the quickCSF algorithm at 16 spatial frequencies for corresponding (left column) and non-corresponding (right column) conditions at 2° (top row) and 6° (bottom row) eccentricities. Boxplots show medians and interquartile range (error bars) of ten observers (2° eccentricity) or 5 observers (6° eccentricity), with left eye and right eye data combined in the monocular data, dots show outliers. Monocular acuities are replotted for comparison in both columns. Significant binocular-monocular contrast sensitivity differences for each spatial Frequency are marked as asterisks, where *=p<0.05; **=p<0.01 and ***=p<0.001.

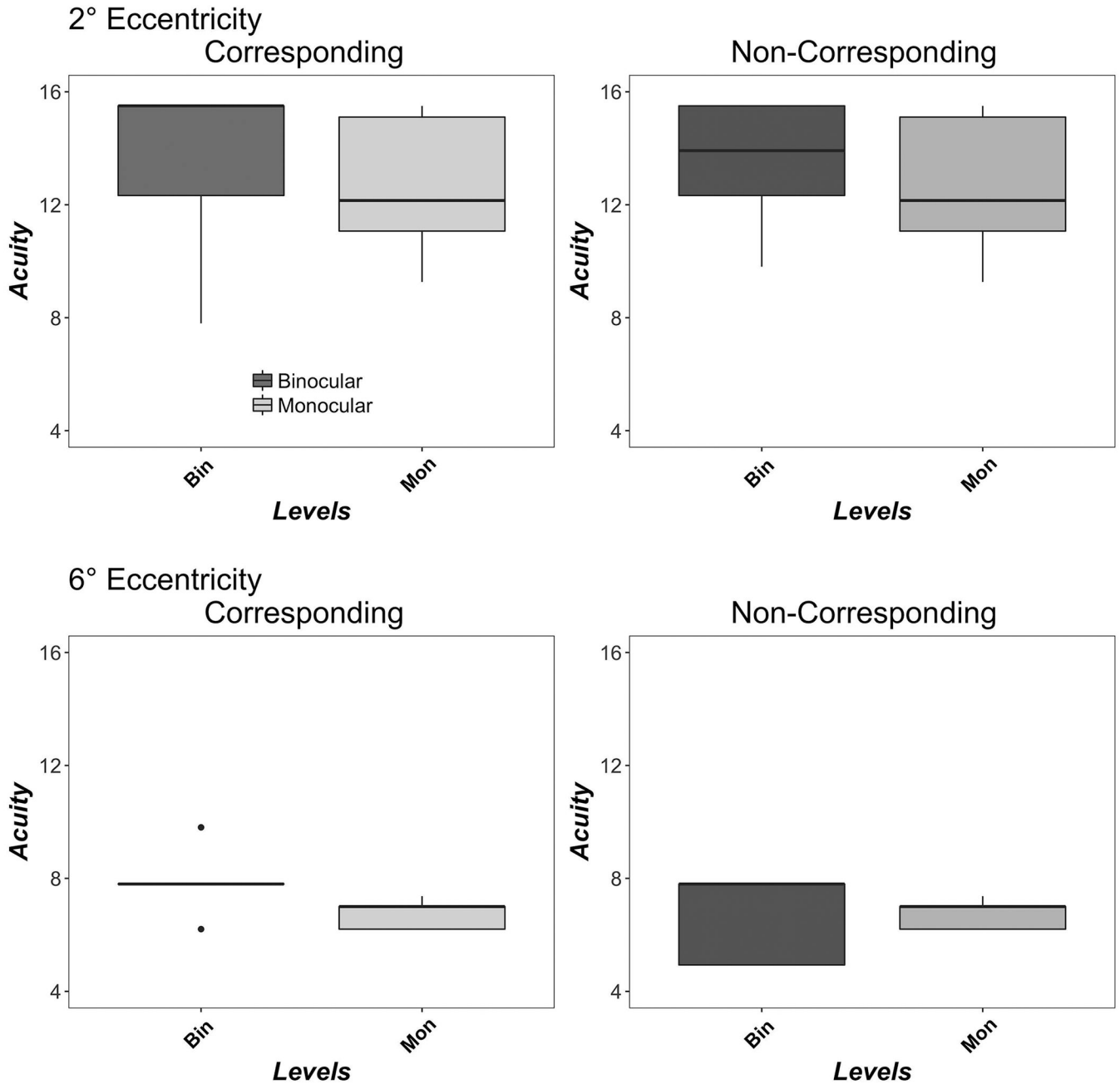


**Figure 2.**

Monocular and Binocular Acuity. Data show CSF Acuity (c/deg) for corresponding (left column) and non-corresponding (right column) Conditions at 2° (top row) and 6° (bottom row) eccentricities. Boxplots show medians and interquartile range (error bars) of ten observers (2°) or five observers (6°), with left eye and right eye data combined in the monocular data, dots show outliers. Monocular acuities are replotted for comparison in both columns.

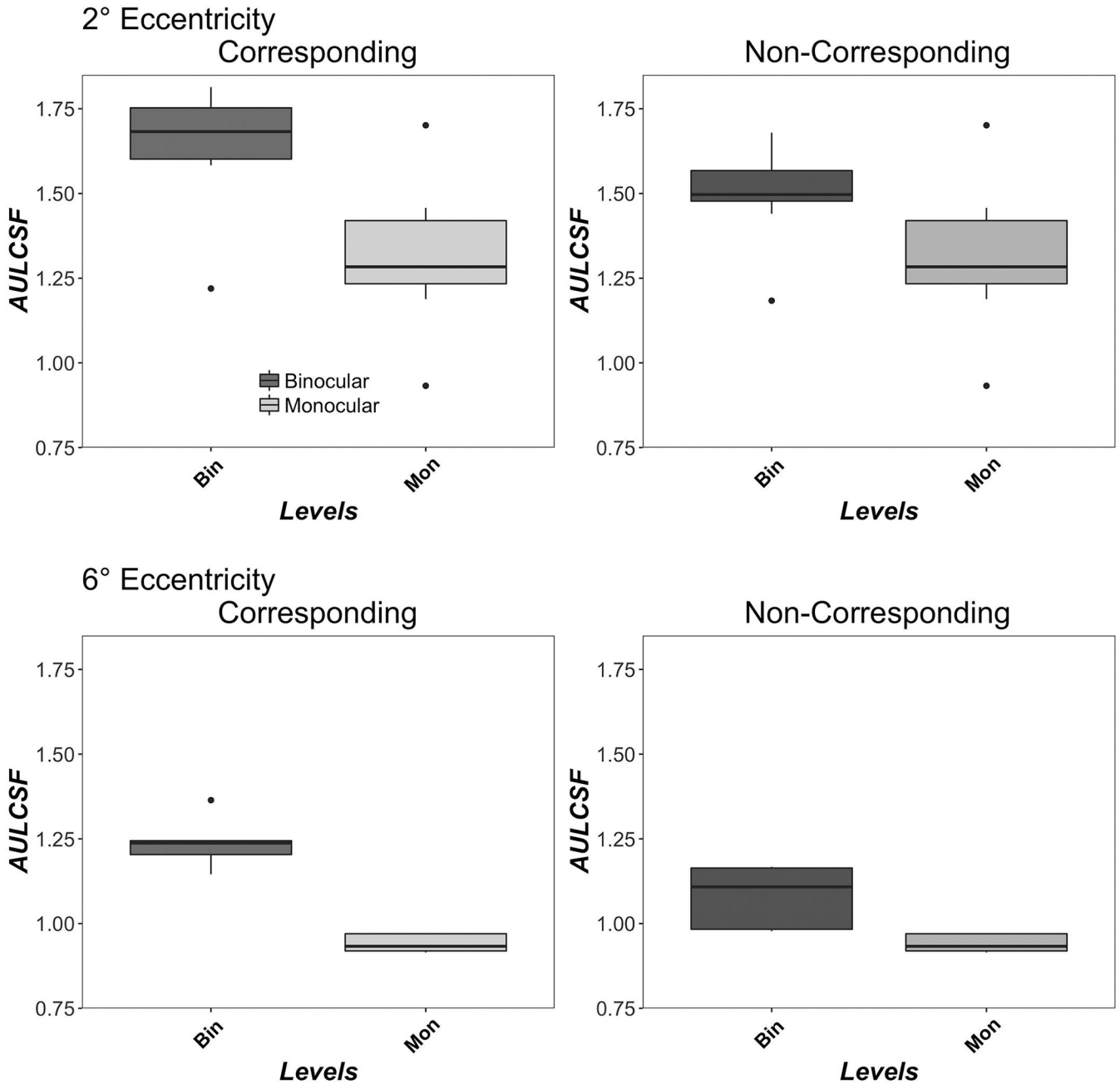


**Figure 3.**

Monocular and Binocular AULCSF. Data show AULCSF for corresponding (left column) and non-corresponding (right column) conditions at 2° (top row) and 6° (bottom row) eccentricities. Boxplots show medians and interquartile range (error bars) of ten observers (2°) or five observers (6°), with left eye and right eye data in the monocular data, dots show outliers. Monocular AULCSF is replotted for comparison in both columns.

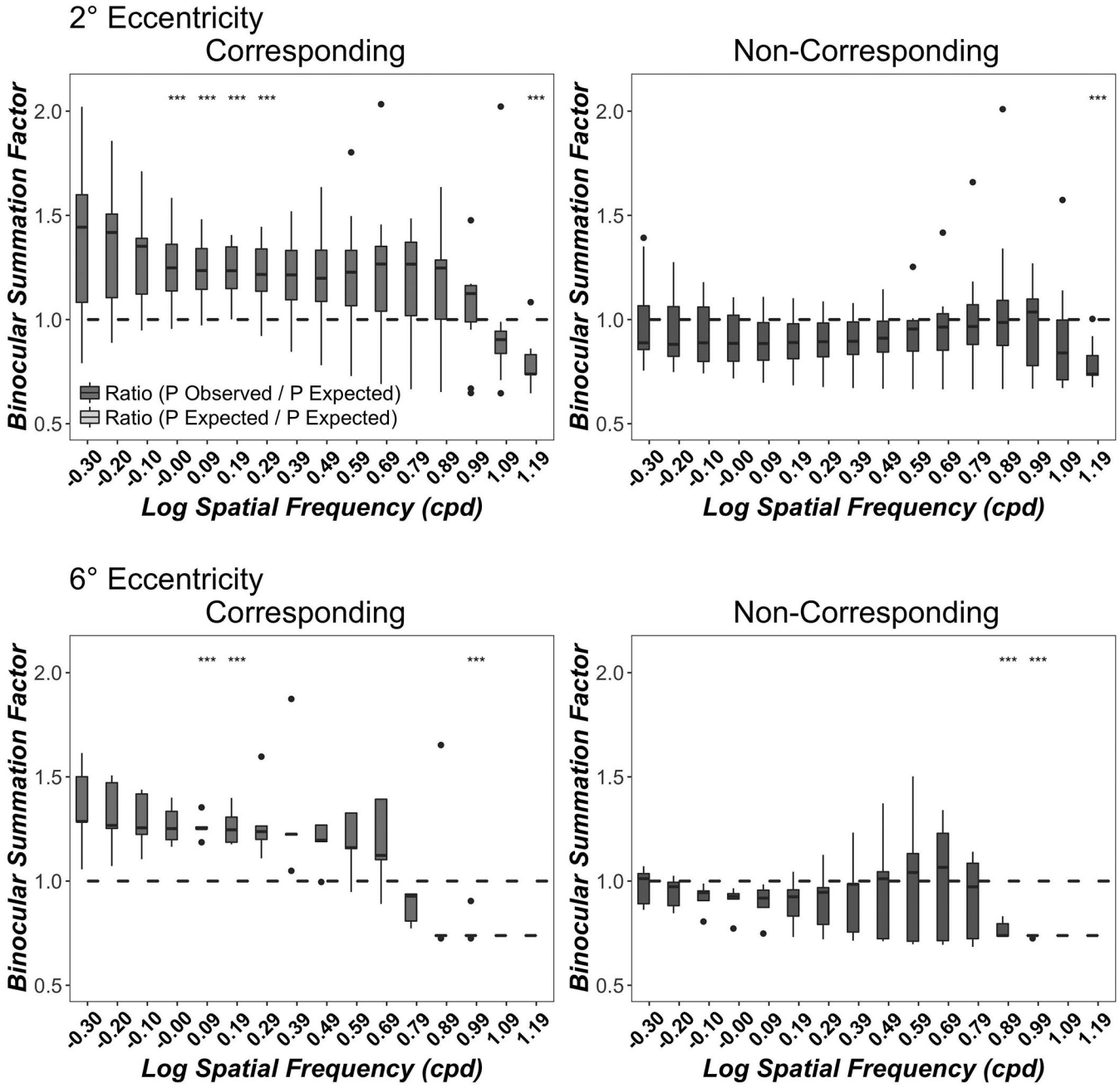


**Figure 4.**

Binocular Contrast Summation as a function of Spatial Frequency. Data show the ratio of observed binocular probability summation over expected binocular probability summation ($P_{Observed\ \text{Binocular}} / P_{\text{Expected binocular}}$) at 16 spatial frequencies for corresponding (left column) and non-corresponding (right column) conditions at 2° (top row) and 6° (bottom row) eccentricities. A value of 1 indicates simple probability summation between independent monocular sensors while a value greater than 1 or lower than 1 indicates a binocular integration mechanism or a binocular inhibition mechanism respectively. Boxplots show medians and interquartile range (error bars) of ten observers (2° eccentricity) or 5

observers (6° eccentricity). The dots are outlier points. Significant binocular contrast summation/inhibition vs probability summation t-tests for each spatial frequency are marked as asterisks.

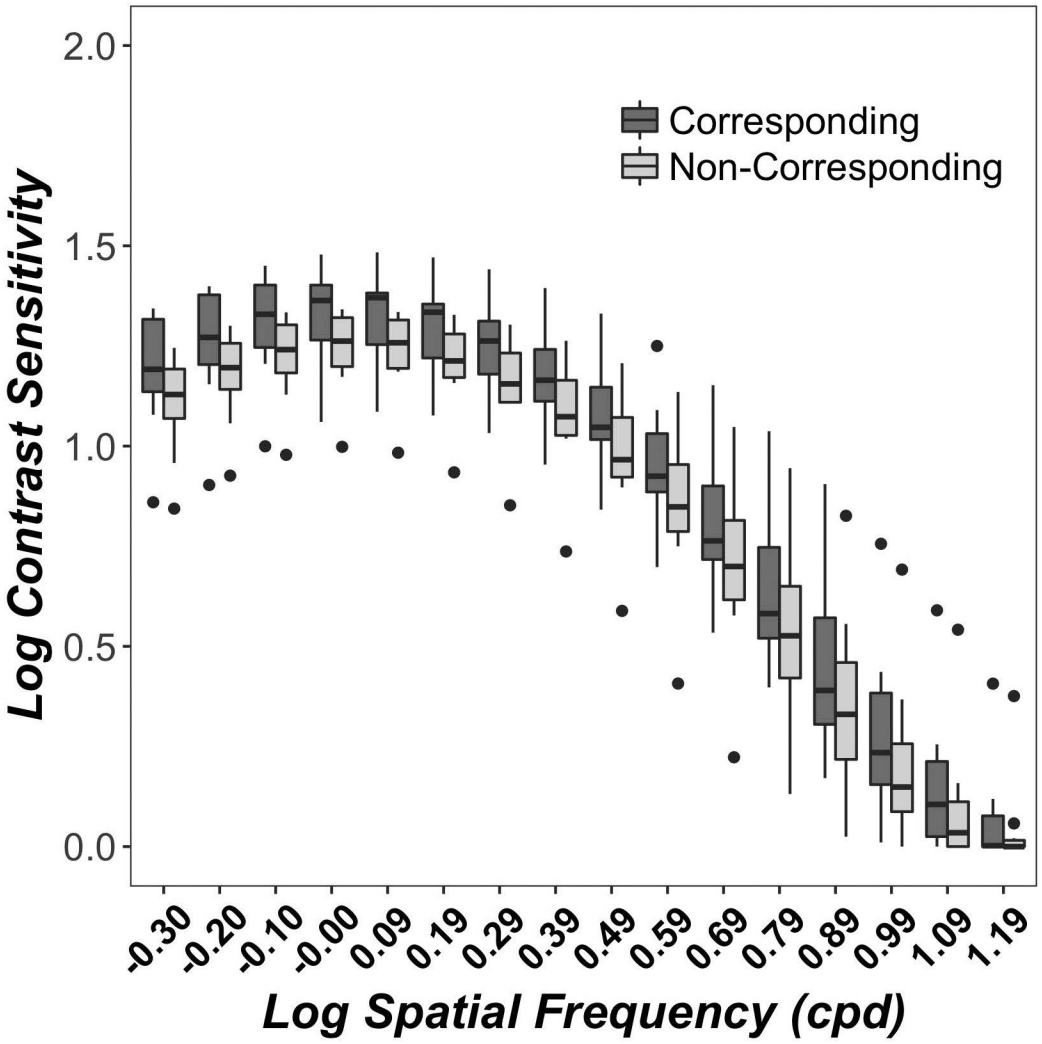


**Figure 5.**
Contrast sensitivity functions for stimuli presented monocularly in binocular corresponding and non-corresponding conditions. Boxplots show medians and quartiles (error bars) of 10 observers. The dots are outlier points.

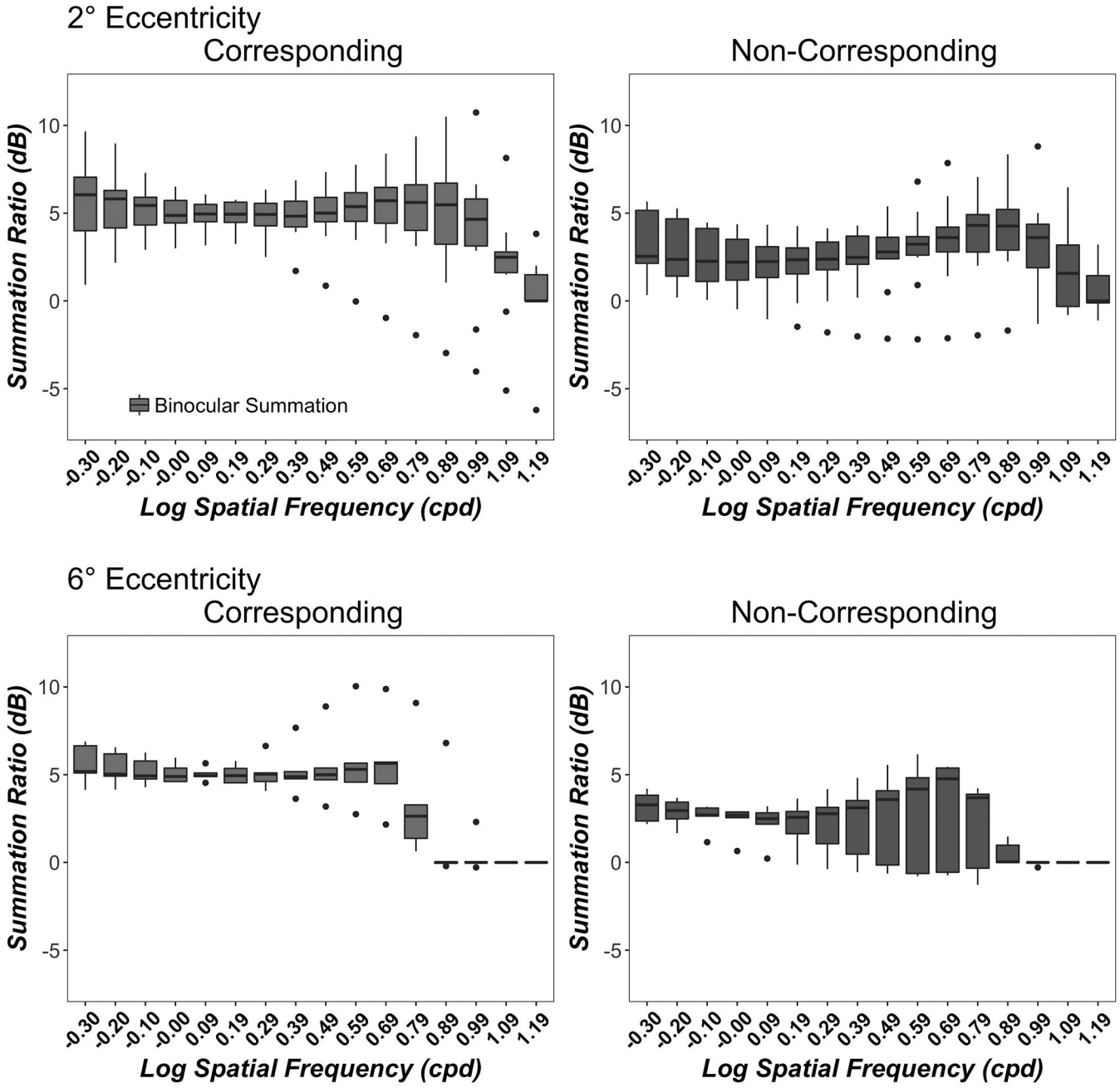


**Figure A1.**

Contrast Summation Ratio as a function of Spatial Frequency. Data show the summation ratio (in dB) between the monocular and the binocular thresholds at 16 spatial frequencies for corresponding (left column) and non-corresponding (right column) conditions at 2° (top row) and 6° (bottom row) eccentricities. Boxplots show medians and interquartile range (error bars) of ten observers (2° eccentricity) or 5 observers (6° eccentricity). The dots are outlier points.